Numerical modelling of detonation reaction zone of nitromethane by EXPLO5 code and Wood and Kirkwood theory

Štimac, Barbara; Chan, Hay Yee Serene; Kunzel, Martin; Sućeska, Muhamed

Source / Izvornik: **Central European Journal of Energetic Materials, 2020, 17, 239 - 261**

Journal article, Published version
Rad u časopisu, Objavljena verzija rada (izdavačev PDF)

https://doi.org/10.22211/cejem/124193

Permanent link / Trajna poveznica: https://urn.nsk.hr/urn:nbn:hr:169:922530

Central European Journal of Energetic Materials
ISSN 1733-7178; e-ISSN 2353-1843

Cent. Eur. J. Energ. Mater. 2020, *17*(2): 239-261; DOI 10.22211/cejem/124193
Article is available in PDF-format, in colour, at:
http://www.wydawnictwa.ipo.waw.pl/cejem/Vol-17-Number2-2020/CEJEM_01112.pdf

Research paper

Numerical Modelling of Detonation Reaction Zone of Nitromethane by EXPLO5 Code and Wood and Kirkwood Theory

Barbara Štimac*[,1], Hay Yee Serene Chan[2], Martin Kunzel[3], Muhamed Suceska[1]

[1] *Faculty of Mining, Geology and Petroleum Engineering, University of Zagreb, Croatia*
[2] *Energetics Research Institute, Nanyang Technological University, Singapore*
[3] *OZM Research, s.r.o., 538 62 Hrochuv Tynec, Czech Republic*
* *E-mail:* bstimac@rgn.hr

Abstract: The detonation reaction zone of nitromethane (NM) has been extensively studied both experimentally and theoretically. The measured particle velocity profile of NM shows the existence of a sharp spike followed by a rapid drop over the first 5-10 ns (fast reaction). The sharp spike is followed by a gradual decrease (slow reactions) which terminate after approximately 50-60 ns when the CJ condition is attained. Based on experimental data, the total reaction zone length is estimated to be around 300 μm. Some experimental observations, such as the reaction zone width and the diameter effect, can be satisfactorily reproduced by numerical modelling, provided an appropriate reaction rate model is known.

Here we describe the model for numerical modelling of the steady state detonation of NM. The model is based on the coupling thermochemical code EXPLO5 with the Wood-Kirkwood detonation theory, supplemented with different reaction rate models. The constants in the rate models are calibrated based on experimentally measured particle velocity profiles and the detonation reaction zone width. It was found that the model can describe the experimentally

measured total reaction time (width of reaction zone) and the particle velocity-time profile of NM. It was found also that the reaction rate model plays a key role on the shape of the shock wave front. In addition, the model can predict the detonation parameters (*D, p_{CJ}, T_{CJ}, V_{CJ}, etc.*) and the effect of charge diameter on the detonation parameters.

Keywords: nitromethane, reaction zone, particle velocity, EXPLO5, Wood and Kirkwood theory

1 Introduction

Nitromethane (NM) is extensively studied as an example of a liquid homogenous explosive. Such explosives contain no voids and therefore there is no hot spot formation during shock compression. Hence, the initiation of homogeneous explosives is governed completely by the strong compression of a thin layer of explosive and obeys temperature-dependent reaction rate laws [1-3]. By adding small amounts of impurities or additives, the initiation properties may be changed from homogenous to those characteristic of heterogeneous explosive [4].

The detonation reaction zone (DRZ), which represents the spatial distance between the von Neumann spike and the sonic locus (or CJ point in the case of ideal explosives) [5], is difficult to determine quantitatively. The reasons for this are: the necessity for experimental techniques with high time resolution and uncertainty in identifying the CJ state from the reaction zone profile [3]. Different experimental techniques are used for direct or indirect measurements of the DRZ; such as the flying plate test, the detonation front curvature test, emitted light measurements and the impedance window technique [4, 6-10]. Since the requirement for a successful experiment is high time resolution, laser velocity interferometry has proven to be one of the most useful and reliable measurement methods. In impedance window experiments, a block of transparent material ("window") is attached to the front surface of a cylindrical explosive charge and the velocity of the interface is measured through the window. This technique provides particle velocity-time profiles that make it directly applicable to the measurement of the DRZ width. Depending on the type of measuring system (Fabry-Perot, VISAR, ORVIS, PDV), the time resolution of laser interferometry methods ranges from 10 ns to less than 1 ns [6-10].

While most experimental studies report the existence of faster and slower chemical reactions in NM DRZ, the width of the zone reported in the literature varies from several tenths to several hundred microns [4, 8, 11-13]. Based on NM shock front curvature measurements, Engelke and Bdzil [11]

estimated a DRZ width of around 36 μm (~6 ns). Recent experiments of Sheffield *et al.* [8], Bouyer *et al.* [7], Mochalova *et al.* [4], performed using laser-based interferometry to measure particle velocity profiles of the steady state detonation wave at the NM/PMMA interface, confirmed the existence of the von Neumann spike, fast reactions that last 5-10 ns and slow reactions that end at the CJ point after 50-60 ns. The time resolution in these studies was 1 ns, rendering these experiments the most relevant studies on NM DRZ so far. The authors estimated the DRZ width of NM to be approximately 50-60 ns (300 μm) [4, 8].

In most experiments, the particle velocity at the von Neumann spike is measured at the NM/PMMA interface [4, 7, 8] and ranges from 2.2 to 2.5 mm/μs. The measured values of particle velocity are 10 to 20% below that theoretically estimated, which is associated with the limitation of measurement techniques to capture particle velocity exactly at the von Neumann spike, but only at some distance behind it. Theoretical calculations, on the other hand, place the particle velocity at the von Neumann spike closer to 3.0 mm/μs [3].

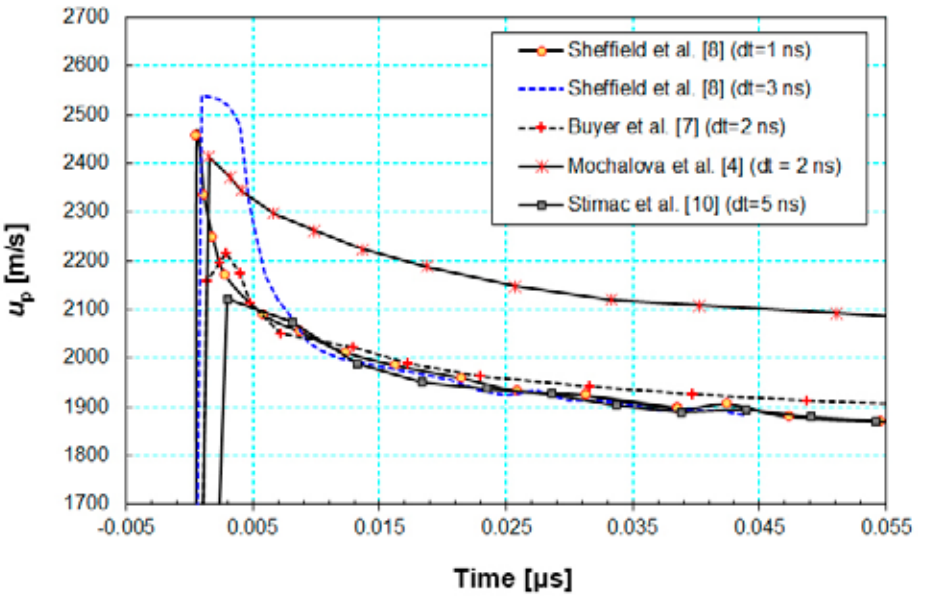

Figure 1. Examples of experimental NM/PMMA interface particle velocity profiles

Some researchers have applied numerical modelling to reproduce the experimentally observed shock initiation behaviour and to resolve the DRZ

structure [1, 3, 14, 15]. The modelling requires the incorporation of a reaction rate equation in the hydrodynamic flow equations, along with the equation of state of the reacted and unreacted explosive in the numerical model. Tarver and Urtiew [1] and Sugiyama *et al.* [14] modelled the steady state detonation of NM in a hydrodynamics code using the ignition and growth reaction rate model and the Jones-Wilkins-Lee (JWL) equation of state for reacted and unreacted NM. This rate model made it possible to reproduce the experimentally observed total reaction time and failure diameters of NM under strong and weak confinement. However, because the initiation of NM as a homogeneous explosive is governed by strong compression (with no hot-spots formation) and has a temperature-dependent reaction rate, most authors use the Arrhenius reaction rate model. Partom [15] described a model based on the reactive flow equations and the first-order Arrhenius reaction rate equation, with the activation energy (E_a) of 222.8 kJ/mol and a pre-exponential factor (A) of $5 \cdot 10^{14}$ s^{-1}. The model was used for shock initiation studies of NM. Hardesty [2] found that $E_a = 95.6$ kJ/mol and $A = 2.6 \cdot 10^9$ s^{-1} better reproduced NM shock initiation experiments. Both Partom's and Hardesty's values of the activation energy are lower than the activation energy for gas phase decomposition of NM (which equals 246.9 kJ/mol and corresponds to breaking of C–N bonds [3]). This is evidence of the existence of different mechanisms for gas-phase and liquid-phase reaction [3].

To model both shock initiation and steady state detonation, Nunziato and Kipp [16] ran in parallel a two-phase reactive flow model and the reaction rate model that describes two reaction mechanisms. The first mechanism dominates at low temperatures (to describe shock initiation, with $E_a = 119$ kJ/mol) and the second mechanism dominates at high temperatures (to describe steady state detonation, with $E_a = 246.9$ kJ/mol). For mesoscale simulation of hot-spot initiation of NM, Menikoff and Shaw [3] developed a model that used **a** second-order Arrhenius reaction rate equation with $E_a = 124.7$ kJ/mol and $A = 1.5 \cdot 10^9$ s^{-1}. The model satisfactorily reproduces Sheffield *et al.* [8] experimental particle velocity-time profiles. Several publications (*e.g.* [3, 15, 16]) show that there is considerable uncertainty in both the reaction rate models and the parameters in the models. The problem of finding the best reaction rate model is complicated by the fact that a small quantity of additives can affect the rate significantly [4]. In this work, we describe a model based on the Wood-Kirkwood (WK) detonation theory coupled with the thermochemical code EXPLO5.

2 Description of the Model

To model the steady-state detonation of NM we coupled the EXPLO5 thermochemical code [10, 17, 18] with the slightly divergent detonation WK theory [19, 20]. The WK theory starts with Euler's hydrodynamic flow equations coupled with chemical kinetics. It considers a cylindrical explosive charge of infinite length and solves the flow equations along the central streamline of the cylinder. The theory treats radial expansion as a first order perturbation to a perfect one-dimensional flow along the streamline and predicts the detonation velocity to be both a function of the chemical reaction rates and the rate of radial expansion. The theory results in a set of ordinary differential equations (ODEs) that describe the hydrodynamic variables and the chemical concentrations of reactant and products along the centre of the cylinder [22]. If the radial expansion term is omitted, the WK equations become identical to the ZND flow equations [5], which consider one-dimensional flow and always predicts the same value for the detonation velocity as the Chapman-Jouguet (CJ) theory.

In our model the WK ODEs are integrated in a separate subroutine, while EXPLO5 calculates the concentration and thermodynamic parameters of the products, and the energy and energy derivatives for a given conversion, pressure and density along the Rayleigh line (Figure 2). The shock wave structure behind the shock front is obtained by integration of the WK equations. The distance (x) behind the shock is related to the time after a Lagrangian particle reaches the shock (t) by the equation:

$$dx = u \cdot dt$$

where u is the axial particle velocity in the moving frame. The initial conditions for the WK ODEs are the state variables (pressure, density, energy, and the reacted fraction of explosive) at the shock front, *i.e.* at the von Neumann spike ($t = 0$). The outputs of the calculation are the steady-state self-sustaining detonation parameters and the flow parameters behind the shock front.

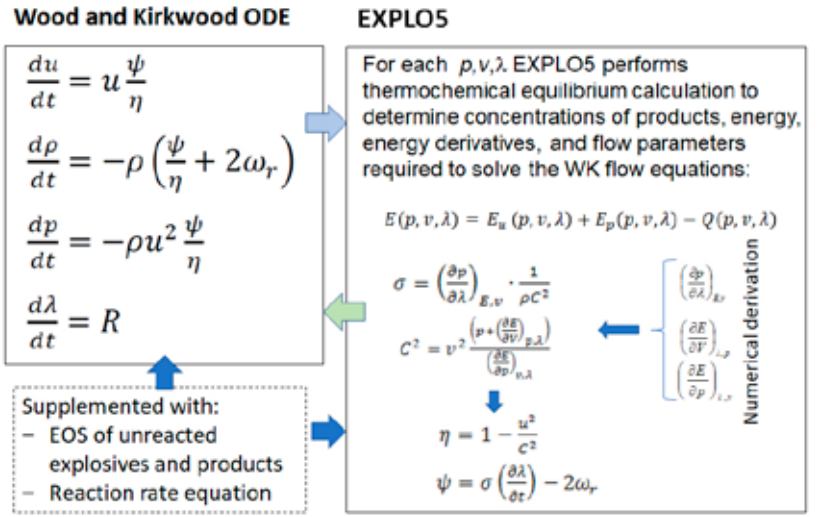

Figure 2. Schematic presentation of the model [17]

In addition, the model is supplemented with the following input information:

– the reaction rate equation for decomposition of the explosive ($d\lambda/dt$),
– the equations of state of the unreacted explosive and the detonation products,
– the thermodynamic functions of the reactants and products as a function of temperature,
– the rate of radial expansion (ω_r).

The state of the gas phase products is described by the Becker-Kistiakowsky-Wilson (BKW) equation of state which is incorporated in EXPLO5 [17]. The states of the unreacted explosive and the condensed detonation products are described by the Murnaghan equation of state which has the form [21]:

$$p = \frac{1}{\kappa n}\left[\left(\frac{V_0}{V}\right)^n - 1\right] \tag{1}$$

where V_0 is the molar volume of a product when $p = 0$, κ is the inverse of the bulk modulus and n is pressure derivative of the bulk modulus.

The rate of radial expansion (ω_r) along the centre streamline of the flow is estimated by the equation proposed by Wood and Kirkwood [19]:

$$\omega_r = (D - u)/R_c \tag{2}$$

which relates the radial expansion rate with the shock front curvature radius (R_c)

and the particle velocity in the shock frame (*u)*.

The thermodynamic functions of the unreacted explosive and detonation products in their standard states are expressed through enthalpy, and the dependence of enthalpy on temperature is described by a 4th degree polynomial [17]. Our model supports several reaction rate models. As mentioned before, the Arrhenius reaction rate model seems a logical choice for NM as it is a homogeneous explosive. This model, which takes into account the conversion and temperature dependence of the reaction rate, is used in the following form [2, 3, 15]:

$$\frac{d\lambda}{dt} = k\lambda^B(1-\lambda)^C \exp\left(\frac{-T_a}{T}\right) \tag{3}$$

where k is the rate constant, λ is the mass fraction of reacted explosive (conversion), T_a is the activation temperature ($T_a = E_a/R$), B and C are constants, and E_a is the activation energy.

A pressure-based reaction rate model assumes the rate is function of conversion and pressure and it is given by Equation 4 [22]:

$$\frac{d\lambda}{dt} = k\lambda^B(1-\lambda)^C p^D \tag{4}$$

where p is the pressure in GPa.

To include the dependence of the reaction rate on pressure in the Arrhenius reaction rate equation, the term p^D is added to Equation 3. Thus, a temperature- and pressure-based reaction rate model can be obtained:

$$\frac{d\lambda}{dt} = k\lambda^B(1-\lambda)^C \exp\left(\frac{-T_a}{T}\right)\ p^D \tag{5}$$

We also tested the applicability of a three-terms ignition and growth (I&G) pressure-based rate model [1]:

$$\frac{d\lambda}{dt} = I(1-\lambda)^b\left(\frac{\rho}{\rho_0} - 1 - a\right)^x + G_1(1-\lambda)^c\lambda^d p^y + G_2(1-\lambda)^e\lambda^g p^z \tag{6}$$

$$0 < \lambda < \lambda_{\text{igmax}} \quad | \quad 0 < \lambda < \lambda_{\text{G1max}} \quad | \quad \lambda_{\text{G2min}} < \lambda < 1$$

where ρ is the current density, ρ_0 is the initial density, and I, G_1, G_2, a, b, c, d, e, g, x, y, and z are constants.

3 Results and Discussion

The aim of our work was to investigate the capability of our model to reproduce the experimentally observed behaviour of NM. Experimental data that are used to validate the model include the detonation velocity, the pressure, and the reaction zone particle velocity-time profiles. For this purpose, we have used Sheffield *et al.*'s [8] experimental data which are considered to be the most relevant published so far. Sheffield *et al.*'s experiments involved measurements of the particle velocity-time history at an NM/PMMA window interface. In these experiments, when the detonation wave reaches the PMMA window, a shock is created which travels into the PMMA, while a reflected shock wave will travel back into the detonation products. Since conservation laws must operate at the interface, the pressure and the particle velocities at the interface are the same in both the NM and PMMA. Thus, equating the Hugoniots of NM and PMMA one can calculate the pressure and particle velocity at the interface. A graphical solution of this interaction problem is illustrated by so-called cross-plot [7, 8] given in Figure 3. To determine the parameters in NM CRZ, the equation of states of both the unreacted NM and its detonation products must be known. To construct the cross plot, we used the following input data:

– the Hugoniot curve of unreacted NM is calculated using the equation $U_s = C + S \cdot u_p$, where $C = 1.76$ mm/μs and $S = 1.56$ [8],
– the Hugoniot of the PMMA is calculated using the equation $U_s = C + S \cdot u_p$, where $C = 2.598$ mm/μs, $S = 1.516$; the density used was 1.186 g/cm^3 [23],
– the Rayleigh line ($p = \rho_0 D u_p$) of NM is calculated using the experimentally determined detonation velocity of $D = 6.3$ mm/μs at $\rho_0 = 1.13$ g/cm^3) [24],
– the Hugoniot of the NM detonation products is approximated by the quadratic function: $p = 1.5434 \cdot u_p^2 + 1.7139 \cdot u_p + 4.7665$, derived based on EXPLO5 calculations results [10].

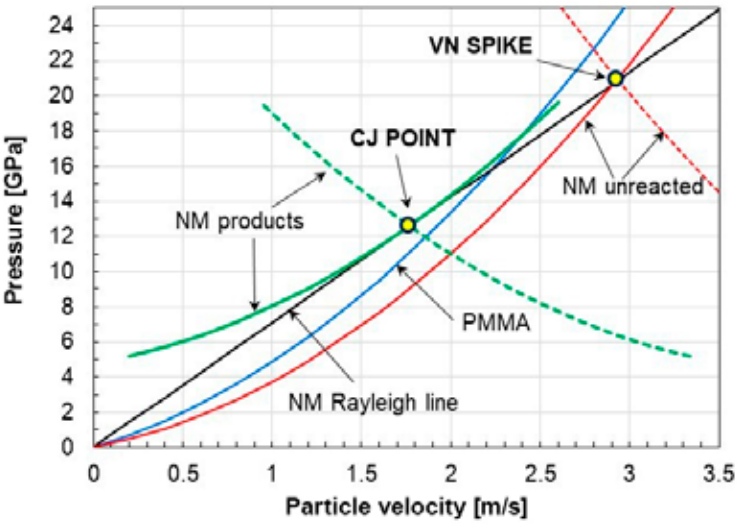

Figure 3. Cross plot of Hugoniots of unreacted NM and its detonation products, Rayleigh line for NM, and Hugoniot of PMMA [10]

Using the cross plot, the particle velocity at the CJ state and at the von Neumann spike at the PMMA/NM interface and in NM are determined. The particle velocity and pressure at the von Neumann spike are determined from the intersection of the Rayleigh line and the Hugoniot of unreacted NM ($u_{p,VNS}$ = 2.925 mm/μs, p_{VNS} = 20.73 GPa). The particle velocity and pressure transferred to the PMMA window are determined from the intersection of the Hugoniot of PMMA and that of unreacted NM. These values ($u_{p,VNS\_NM/PMMA}$ = 2.78 mm/μs, $p_{VNS\text{-}NM/PMMA}$ = 21.02 GPa) should correspond to values measured experimentally at the NM-PMMA interface. The CJ point is determined from the intersection of the NM Rayleigh line and the Hugoniot of the detonation products ($u_{p,CJ}$ = 1.77 mm/μs, p_{CJ} = 12.6 GPa), while the particle velocity corresponding to the CJ state transferred to the PMMA window is determined from the intersection of the Hugoniots of the PMMA Hugoniot and the detonation products ($u_{p,CJ,NM/PMMA}$ = 1.86 mm/μs, $p_{CJ,NM/PMMA}$ = 12.1 GPa).

The model described earlier in the text calculates the state variables at the von Neumann spike and behind it down to the CJ/sonic point, and the self-sustaining steady-state detonation velocity, in the following way:

– The Wood-Kirkwood equations are integrated by applying the Runge-Kutta method. The integration starts at the von Neumann spike and continues toward the CJ/sonic point.
– The detonation velocity is treated as a known (specified) parameter.

The intersection of the Rayleigh line for a specified detonation velocity with the shock Hugoniot of the unreacted explosive gives the von Neumann spike and values for the corresponding pressure and volume (p_{VNS}, v_{VNS}).

– For a given p, v, and λ along the Rayleigh line, EXPLO5 calculates the concentrations of the products and the energy:

$$E(p, v, \lambda) = E_u(p, v, \lambda) + E_p(p, v, \lambda) - Q(p, v, \lambda)$$

where the subscripts u and p mean unreacted explosive and reaction products, respectively.

– The initial reacted fraction of explosive ($\lambda_{(t=0)}$) is taken to be close to zero (0.5%). The conversion as a function of time ($\lambda(t)$) is calculated by the integration of a reaction rate equation using the Runge-Kutta method.

– The self-sustaining steady-state detonation velocity is obtained by varying the detonation velocity until two conditions are satisfied simultaneously:
  a) the flow is sonic and
  b) the release of energy by chemical reactions is balanced by the energy loss by radial flow [19, 22].

  This is done by applying the minimisation method described by Fried *et al.* [22].

– The state of the unreacted NM is described by the Murnaghan equation of state (Equation 1). The parameters in the Murnaghan equation of state for NM are:
  a) $V_0 = 54.02$ cm^3/mol,
  b) $\kappa = 5.03 \cdot 10^{-5}$ 1/bar,
  c) $n = 6.97$.

  These values are derived from the linear U_s-u_p dependence ($U_s = C + S \cdot u_p$, where $C = 1.76$ mm/μs and $S = 1.56$) [8].

– The thermodynamic functions of unreacted NM are derived from the heat capacity *vs*. temperature values reported by [25]. The dependence of enthalpy on temperature is described by a fourth-degree polynomial.

– The detonation products include: H_2O, N_2, H_2, NH_3, CO_2, CO, CH_4, CH_2O_2, and $C_{(gr)}$.

– Input parameters for the explosive: NM sensitized by 1% of ethylene diamine having density 1.128 g/cm^3, unconfined explosive charge, charge diameter 25 mm, failure radius 2 mm, radius of shock curvature 104 mm (calculated by Souers' empirical equation [22]).

In addition to the equations of state and the thermodynamic functions of the unreacted explosive and its detonation products, the rate of decomposition

of the explosive has a crucial impact on the calculation accuracy of the chemical reaction zone profile. We tested the capability of several rate models to describe Sheffield *et al.*'s [8] experimentally measured particle velocity profiles. The models include:

– a simple pressure-based model,
– temperature-based model (Arrhenius reaction rate),
– a temperature- and pressure-based model and
– an ignition and growth model.

The calibration of the constants in the models is performed by fixing the reaction rate order (first or second) and the pressure exponent (between 1 and 2) and adjusting the rate constant so to reproduce the total reaction time of 55 ±5 ns, reported by Sheffield *et al.* [8]. The activation temperature (T_a) in the Arrhenius reaction rate models is taken to be 15000 K (after Menikoff and Shaw [3]), which corresponds to an activation energy of 124.7 kJ/mol. For the I&G model, the rate constants are taken from Tarver and Urtiew [1]. The rate constants used are summarised in Table 1. The calculation has shown that using these adjusted rate constants, all the tested rate models give practically the same parameters at the von Neumann spike and the CJ/sonic point – the difference being less than 0.5%. The calculated parameters at the von Neumann spike and at the CJ/sonic point are given in Tables 2 and 3.

Table 1. Reaction rate models used and rate constants used in calculations

Model denotation	Type of reaction rate model	Constants in rate equations
TB-C1	1st order Arrhenius reaction rate model (Equation 3)	k = 30000 1/μs, B = 0, C = 1, T_a = 15000 K
TB-C2	2nd order Arrhenius reaction rate model (Equation 3)	k = 255000 1/μs, B = 0, C = 2, T_a = 15000 K
PB-C1D2	Pressure-based model, C=1 (1st order) (Equation 4)	k = 0.47 1/ (μs GPa^D), B = 0, C = 1, D = 2
PB-C1.7D2	Pressure-based model, C=1.7 (1.7th order) (Equation 4)	k = 4.6 1/ (μs GPa^D), B = 0, C = 1.7, D = 2
TPB-C2D1	Temperature- and pressure-based model (2nd order) (Equation 5)	k = 13000 1/(μs GPa^D), B = 0, C = 2, D = 1, T_a = 15000 K
TPB-C2D2	Temperature- and pressure-based model (2nd order) (Equation 5)	k = 1100 1/(μs GPa^D), B = 0, C = 2, D = 2, T_a = 15000 K
I&G	Ignition and growth model (Equation 6)	I = 1000 1/μs, a = 0.5741, b = 0.667, x = 4, G_1 = 121875 1/(μs Mbar^y), c = 0.667, d = 0.667, y = 4, G_2 = 240 1/(μs Mbar^z), e = 0.667, g = 0.667, z = 1, $\lambda_{ig,max}$ = 0.01; $\lambda_{G1,max}$ = 0.8; $\lambda_{G2,min}$ = 0.8

Table 2. Calculated and experimental parameters at the von Neumann spike

Parameter	This work[a]	Menikoff and Shaw [3][a]	Partom [15][a]	Cross-plot, this work	Experimental, Sheffield *et al.* [8][b]
E_{VNS} [MJ/kg]	4262	4511	3629[c]	–	–
$u_{p,VNS}$ [mm/μs]	2.923	3.004	2.700	2.925[a] 2.780[b]	2.450
p_{VNS} [GPa]	20.88	21.11	19.13	20.73 [a] 21.02[b]	–
T_{VNS} [K]	1.603	1.872	2.205	–	–
ρ_{VNS} [g/cm^3]	2.0910	2.1659	1.9786	–	–
$C_{o,VNS}$ [mm/μs]	8.373	–	–	–	–

Note: [a] parameters in NM, [b] parameters at NM/PMMA interface, [c] parameter derived using the CJ theory

Table 3. Calculated and experimental detonation parameters for NM at the CJ/sonic point

Parameter in CJ state	Experimental values (ρ =1.128-1.14 g/cm^3)	This work (ρ =1.128 g/cm^3)
D [m/s]	6280, 6300 [24] 6300 [10, 26]	6340
p_{CJ}, [GPa]	12.5 [24] 13.0 [26]	12.30
T_{CJ} [K]	3430 [27] 3400-3800 [3][a]	3198
ρ_{CJ} [g/cm^3]	1.556 [24][a]	1.541
$u_{p,CJ}$ [mm/μs]	1.742 [24][a] 1.750 [7, 8]	1.717
t_{CRZ} [ns]	6 [11] 50 [4, 8] 100-150 [7] 100-180 [13]	51-61 (average 54.5)
w_{CRZ} [μm]	36 [11] ~300 [8] 600-900 [7]	206-264 (average 232)
λ_{CJ}	–	0.9934-0.9999

Note: [a] derived based on the CJ theory

It follows from Table 2 that the calculated parameters at the von Neumann spike are very close to those obtained by Menikoff and Shaw [3]. Larger discrepancies in temperature can be attributed to the differences in the equations of state and in the thermodynamic functions of unreacted NM used by Menikoff and Shaw and in our work, and the same goes for the temperature values at the CJ/sonic point. Due to lower temperatures we are able to obtain the same conversion rate as Menikoff and Shaw using a higher value of the rate constant (Figure 4). The interface particle velocity measured by Sheffield *et al.* [8] equals ~2.45 mm/μs, which is ~12% lower than expected (2.78 mm/μs) from the cross-plot. This difference is a consequence of the insufficient time resolution of the measuring system, which causes the front to be truncated.

For the second-order Arrhenius reaction rate model, Menikoff and Shaw [3] used $k = 1.5 \cdot 10^3$ μs^{-1}, while our calculations show that $k = 2.55 \cdot 10^5$ μs^{-1} best reproduces the total reaction time of 50 ns obtained by Sheffield *et al.* [8]. This is primarily the consequence of the differences between the thermodynamic data for NM and its products used by Menikoff and Shaw and those used by us. This illustrates the sensitivity of the Arrhenius reaction rate models to the thermodynamic properties and equations of state of unreacted NM and its products. Authors adjust the reaction rate constants to reproduce their experimental results based on the equations of state and thermodynamic functions used by the author for reacted and unreacted explosive and therefore may vary from author to author.

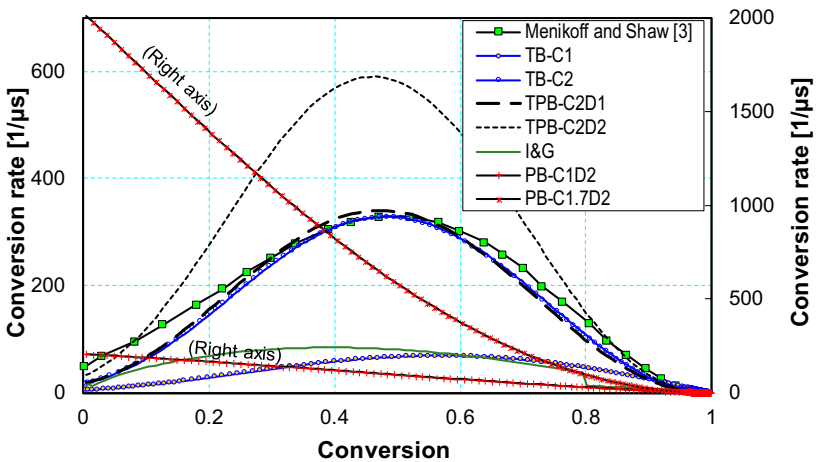

Figure 4. Calculated conversion rates *vs.* conversion for different reaction rate models (conversion rate for pressure-based models is shown on the right vertical axis

Although all reaction rate models tested predict the same total reaction time of 55 ±5 ns, they produce rather different conversion-time and particle velocity-time profiles (Figures 5 and 6). All models, except the pressure-based models, have a sigmoidal λ-t shape characteristic of autocatalytic reactions, with maximum conversion rate occurring at about 0.5 conversion (Figure 4), *i.e.* at several nanoseconds, depending on the rate model (Figure 5(b)). This means they will predict the existence of an induction period. On the other hand, the pressure-based models predict higher reaction rates at the beginning of reaction, without any induction period (Figure 5).

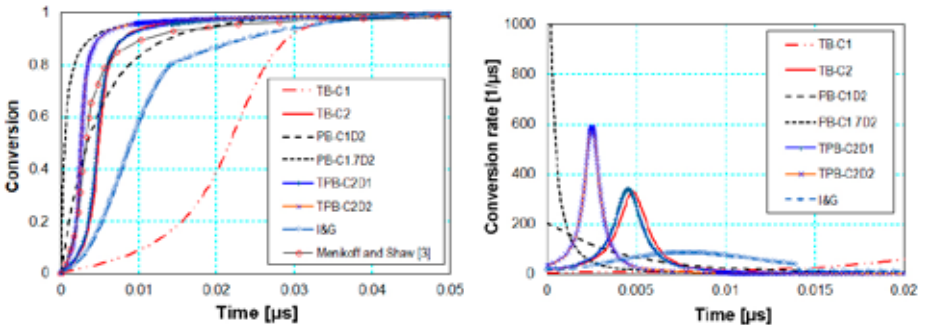

(a) (b)

Figure 5. Calculated conversion-time and conversion rate-time profiles obtained using different reaction rate models

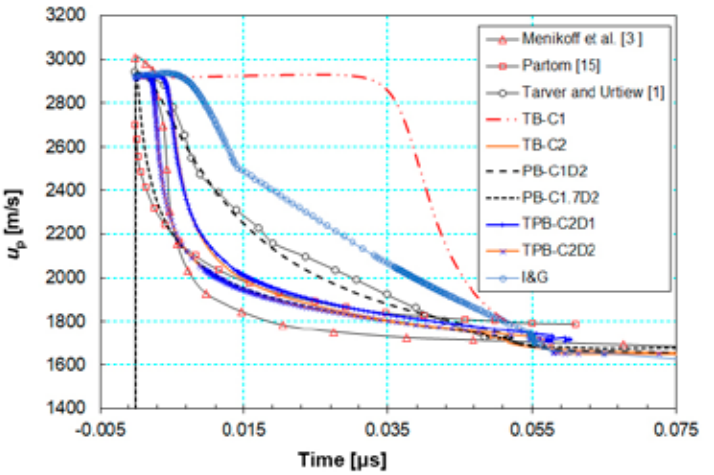

Figure 6. Calculated particle velocity of NM *vs.* time, obtained by different reaction rate models

NM particle velocities profiles calculated using different reaction rate models are given in Figure 6, along with the profiles calculated by some other authors. The pressure-based models do not predict a flat region after the shock front while other models predict the existence of a flat region (induction period) that lasts from a few ns to about 35 ns in the case of the TB-C1 model. The pressure-based model PB-C1.7D2 gives a particle velocity profile similar to that obtained by Partom [15], while our temperature-based model TB-C2 and temperature- and pressure-based model TPB-C2D2 gives a profile similar to that of Menikoff and Shaw (with an induction period of a few ns). Our I&G model gives a slightly different particle velocity profile compared to the profile reported by Tarver and Urtiew [1] obtained by hydrocode calculations. This discrepancy can be due to the differences in the equations of state of reacted and unreacted NM used by Tarver and Urtiew and by us in our calculations. Since Tarver and Urtiew's reported particle velocity refers to the NM/PMMA interface velocity, the values are converted to the NM particle velocity as described below.

The output of our calculations is the NM particle velocity ($u_{p,NM}$). It is related to the NM/PMMA interface particle velocity ($u_{p,NM/PMMA}$) in the way described earlier using the cross-plot (Figure 3). We converted the NM/PMMA interface particle velocity into the NM particle velocity assuming Cooper's generalized isentrope for detonation products [23] is applicable even in the case when the explosive is partially reacted. From the cross-plot we found that the relationship between these two particle velocities can be approximated by a linear function:

$$u_{NM} = 1.6\, u_{p,NM/PMMA} - 1.25$$

where u_p is in mm/μs. Since the Hugoniot curves of PMMA and NM are quite close to each other, this approximation does not significantly affect the accuracy of the calculation results. In this way we converted Sheffield *et al.*'s [8] experimental particle velocities to NM particle velocity in order to validate the calculation results.

Sheffield *et al.* [8] experimentally obtained the reaction zone profiles of detonating NM using two different measuring systems:

– an older "home-made" VISAR system with a time resolution of 3-4 ns,
– a newer VALYN VISAR system with a time resolution of ~1 ns [8].

Using the first measuring system the authors observed the existence of a flat region (induction period) near the shock front, with a duration of 3-4 ns. However, using the second measuring system, with higher time resolution (1 ns), the induction period was not observed. Based on this, the authors concluded that

the existence of the flat region obtained using the older VISAR system was an artefact and the system was not accurately measuring wave shapes [8]. However, both measuring systems showed the spike level at the NM/PMMA interface of about ~2.5 mm/μs and a reaction zone duration of ~50 ns. Based on Sheffield *et al.*'s [8] experimental results it seems either there is no strong evidence of the existence of an induction period or the induction period is too short (on a sub-nanosecond scale). It should be added that Buyer *et al.* [7] and Mochalova *et al.* [4] also did not observe the existence of a flat region after the shock front.

The pressure-based model PB-C1.7D2 better describes the newer measurements of Sheffield *et al.* (time resolution of 1 ns). The model does not predict the existence of an induction period and predicts a very rapid reaction rate immediately after the shock front so that the shape of the shock wave changes rapidly in the first 5-10 ns (after 1 ns 70% of the NM is converted to the products, 93% after 5 ns and 96% after 10 ns) followed by a slow decomposition during the remaining 40 ns.

The temperature- and pressure-based model TPB-C2D2 and the temperature-based model TB-C2 better describes the older measurements of Sheffield's *et al.* These models predict the existence of an induction period of 2-4 ns (Figure 7).

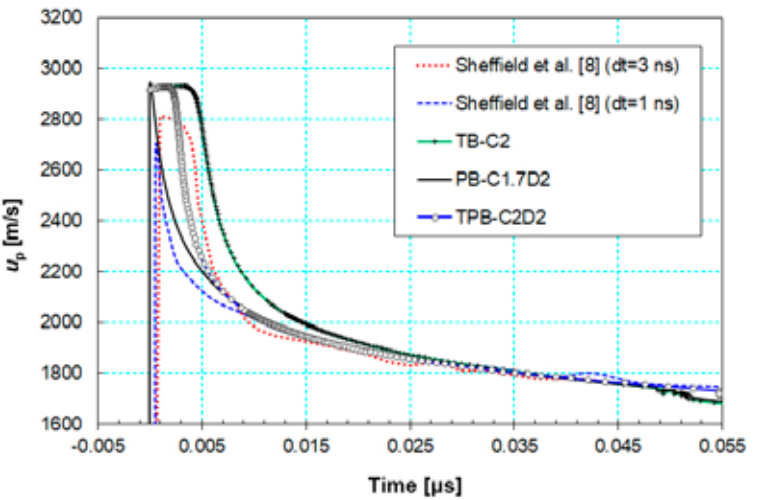

Figure 7. Comparison of calculated and experimental particle velocity profiles of NM

3.1 Detonation reaction zone profile

The NM particle velocity calculated using the PB-C1.7D2 rate model is found to be 2.92 mm/μs at the von Neumann spike and after approximately 1.5 ns drops by about 15% to 2.5 mm/μs. Sheffield *et al.* [8] measured the particle velocity at the von Neumann spike to be ~2.45 mm/μs – which is about 17% lower than calculated. Thus, the von Neumann spike obtained by measurements is truncated, which is the consequence both of the insufficient time resolution of experimental systems and a very sharp drop in the particle velocity in the vicinity of the spike (about 15% after 1.7 ns). This suggests that the experimentally measured spike particle velocity is the velocity at some distance from the von Neumann spike, not at the spike itself.

Since the time resolution of today's measuring techniques is limited, the only way to restore the entire von Neumann spike and detonation reaction zone is by numerical modelling, provided the reaction rate model and parameters are properly calibrated by experiment. Figure 8 illustrates some of the capabilities of our model to calculate the temporal and spatial distribution of the thermodynamic and flow parameters within the reaction zone.

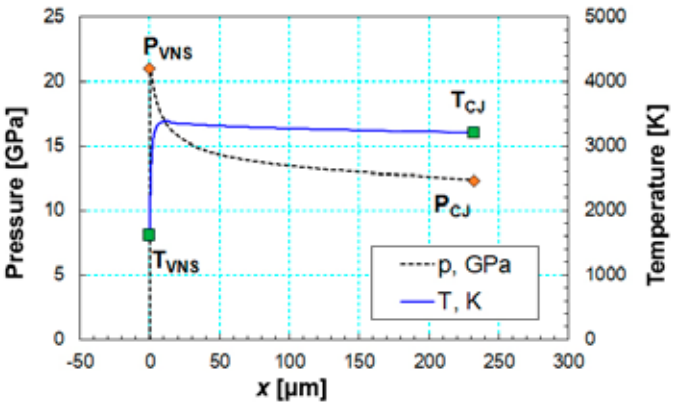

(a)

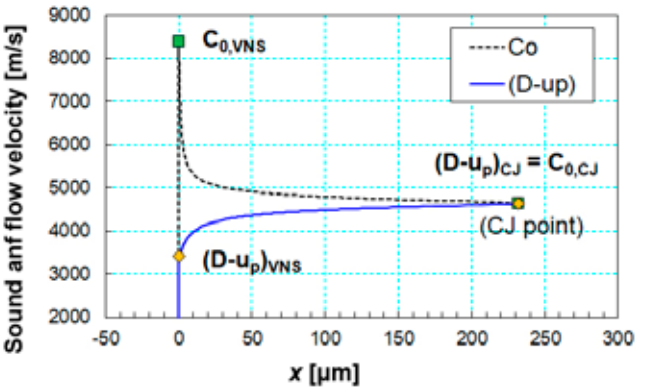

(b)

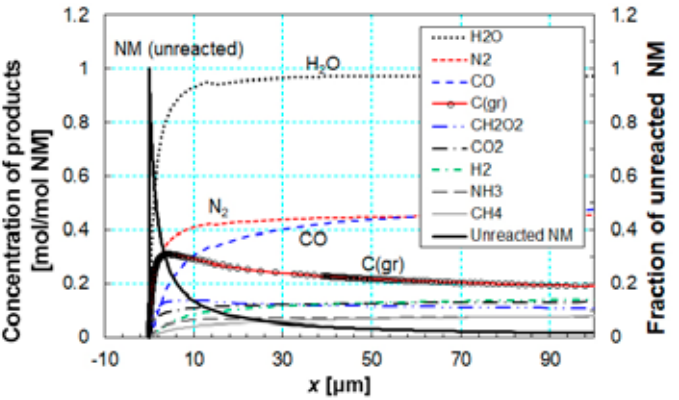

(c)

Figure 8. Spatial distribution of pressure and temperature (a), sound and flow velocity (b), and concentration of products within first 100 µm ns (25) behind the shock (c); calculation done using PB-C1.7D2 rate model

The pressure-based model PB-C1.7D2 predicts rapid decomposition of NM immediately after the shock front and the formation of detonation products. In approximately 10 ns (41 µm), 96% of the NM reacts, while the remaining 4% reacts in a slow process that takes an additional 40 ns. The temperature at the von Neumann spike equals 1603 K and reaches its maximum value of 3391 K after 3.5 ns (14 µm), followed by a small decrease toward the CJ point (3198 K). The model predicts a change of concentration of individual products as the temperature and pressure change within the reaction zone (Figure 8(c)).

In the vicinity of the von Neuman spike, where the pressure is higher and the temperature lower, mole fractions of H_2O, CO_2, CH_2O_2, and C dominate, while CH_4, NH_3, H_2, and CO dominate after 10 ns. Figure 8(b), which shows the change of the sound velocity (C_0) and the flow velocity (D-u_p) behind the shock front, illustrates the fulfilment of the CJ conditions ((D-u_p) = C_0) after 55 ns (232 μm).

It is important to note that the general reaction rate models used in this study represent a simplification of the reactions that take place during NM decomposition. To illustrate this, it was observed experimentally that carbon formation takes approximately 50-60 ns [1], whereas the rate model used in this study predicts carbon formation immediately after the shock front. Tarver and Urtiew's [1] three-term rate law model (I&G model) is designed to describe the three stages of reaction generally observed in shock initiation and detonation. However, it also predicts the immediate formation of carbon. Detailed kinetics, which involve multi-step kinetic models that describe the rates of each individual reaction and process, are required in order to correctly model the concentration of products within the NM reaction zone. Nevertheless, they enable us to reproduce the experimentally observed detonation behaviour of NM with sufficient accuracy.

4 Conclusions

To model the detonation reaction zone of nitromethane we developed the model based on coupling the Wood and Kirkwood detonation theory with the thermochemical code EXPLO5. The model uses the Becker-Kistiakowsky-Wilson equation of state for the gas phase products and the Murnaghan equation of state for unreacted nitromethane and condensed products and supports several reaction rate models. The model can predict steady-state detonation parameters as a function of charge diameter, as well as the temporal and spatial distribution of the thermodynamic and the flow parameters within the detonation reaction zone. The model has been applied to experimental data for nitromethane with satisfactory results – the calculated detonation parameters and the reaction zone profile agree well with those that have been experimentally determined.

The reaction rate parameters are calibrated to reproduce Sheffield *et al.*'s [8] experimentally obtained total reaction time and particle velocity-time profiles. While the total reaction time can be reproduced by all rate models used, the shock wave profile strongly depends on the rate model. The temperature-based as well as temperature- and pressure-based rate models predict the existence

of an induction period (lasting 2-30 ns, depending on the rate model) and they better describe Sheffield *et al.*'s [8] older experimental results obtained using a "home-made" VISAR system (time resolution of 3 ns). The pressure-based reaction rate models do not predict the existence of an induction period and they better describe Sheffield *et al.*'s recent experimental results obtained using a newer VALYN VISAR system (time resolution of 1 ns).

The single-step reaction rate models used in this research represent an oversimplification of the true reactions that take place during detonation of nitromethane. The true reactions are much more complex and their description requires multi-step reaction rate models, that take into account the rates of all individual reactions during the detonation process. Nevertheless, these models are able to reproduce the general phenomena of experimentally observed particle velocity-time profiles such as the existence of a sharp spike followed by a rapid drop over the first 5-10 ns (fast reaction), followed by a slower decrease (slow reactions) which terminates after approximately 50-60 ns when the CJ/sonic condition is attained. The calculated total reaction time equals 51-61 ns (average 54.5 ns), which results in a chemical reaction zone width of 206-264 μm (average 232 μm). This is close to the experimentally measured results of Sheffield *et al.* [8].

The results show that combining an experimentally measured particle velocity-time profile with numerical modelling is a good approach in resolving the reaction zone profile of nitromethane. However, there are still some issues that make it difficult to accurately determine the nitromethane reaction zone structure, both experimentally and by numerical modelling. While experimental measurements give some structural information on the shock wave front, present limitation in the time resolution prevents measurement of the von Neumann spike velocity. To observe the von Neumann spike, time resolution in the sub-nanosecond range is needed in experimentation. Another issue related to measurement is the variability of the shape of the shock wave near the spike, which indicates problems with measurement response during the initial shock rise; *e.g.* see [3, 8].

Besides the reaction rate equation, accurate equations of state of unreacted nitromethane and gaseous and condensed products are required for accurate modelling of the nitromethane reaction zone. In addition, the temperature dependence of thermodynamic functions for unreacted nitromethane and its products plays an important role, particularly when the Arrhenius rate equation is used.

Acknowledgments

This research was supported by the Croatian Science Foundation (HRZZ), Croatia, under the projects IP-2019-04-1618 and I-2243-2017 and the Faculty of Mining, Geology and Petroleum Engineering, Zagreb, Croatia.

References

[1] Tarver, C.M.; Urtiew, P.A. Theory and Modeling of Liquid Explosive Detonation. *J. Energ. Mater.* **2010**, *28*: 299-317.
[2] Hardesty, D.R. An Investigation of the Shock Initiation of Liquid Nitromethane. *Combust. Flame* **1976**, *27*: 229-251.
[3] Menikoff, R.; Shaw, M.S. Modelling Detonation Waves in Nitromethane. *Combust. Flame* **2011**, *158*: 2549-2558.
[4] Mochalova, V.; Utkin, A.; Lapin, S. Detonation Properties of Nitromethane/ Diethylenetriamine Solution. *AIP Conf. Proc.,* **2017**, *1973*: 030005.
[5] Fickett, W.; Davis, W.C. *Detonation: Theory and Experiment*. Dover Publications Inc., Mineola/New York, **1979**, p. 210.
[6] Suceska, M. *Test Methods for Explosives.* Springer-Verlag, New York, **1995**, p. 235.
[7] Bouyer, V.; Sheffield, S.A.; Dattelbaum, D.M.; Gustavsen, R.L.; Stahl, D.B.; Coucet, M.; Decaris, L. Experimental Measurements of the Chemical Reaction Zone of Detonating Liquid Explosives. *AIP Conf. Proc.,* **2009**, *1195*: 177-180.
[8] Sheffield, S.A.; Engelke, R.; Alcon, R.R.; Gustavsen, R.L.; Robins, D.L.; Stacy, D.B.; Whitehead, M.C. Particle Velocity Measurements of the Reaction Zone in Nitromethane. *Int. Detonation Symposium*, *Proc., 12th,* Office of Naval Research, Arlington VA, **2002**, 159-166.
[9] Pachman, J.; Künzel, M.; Nemec, O.; Majzlík, J. A Comparison of Methods for Detonation Pressure Measurement. *Shock Waves* **2018**, *28*: 217-225.
[10] Stimac, B.; Suceska, M.; Kunzel, M.; Stanković, S.; Kucera, J. Detonation Reaction Zone in Nitromethane: Experimental and Numerical Studies. *Seminar New Trends Res. Energ. Mater.*, *Proc., 22nd,* Pardubice, Czech Republic, **2019**, 216-228.
[11] Engelke, R.; Bdzil, J.B. A Study of the Steady-state Reaction-zone Structure of a Homogeneous and a Heterogeneous Explosive. *Phys. Fluids* **1983**, *26*: 1958-1988.
[12] Bdzil, J.B.; Engelke, R.; Christenson, D.A. Kinetics Study of a Condensed Detonating Explosive. *J. Chem. Phys.* **1981**, *74*: 5694.
[13] Koldunov, S.A.; Ananin, V.A.; Garanin, V.A.; Sosikov, V.A.; Torunov, S.I. Detonation Characteristics of Diluted Liquid Explosives: Mixtures of Nitromethane with Methanol. *Combust., Explos., Shock Waves* **2010**, *46*: 64-69.
[14] Sugiyama, Y.; Wakabayashi, K.; Matsumura, T.; Nakayama, Y. Numerical Simulations of the Diameter Effect for Nitromethane Using Ignition and Growth Model. *ICDERS*, *25th,* Leeds, UK, **2015**.

[15] Partom, Y. Revisiting Shock Initiation Modeling of Homogeneous Explosives. *J. Energ. Mater.* **2013**, *31*: 127-142.
[16] Nunziato, J.W.; Kipp, M.E. *Numerical Studies of Initiation, Detonation and Detonation Failure in Nitromethane.* Sandia National Laboratory Report No. SAND81-0669, **1983**.
[17] Suceska, M. *EXPLO5 User's Guide.* OZM Research s.r.o., Hrochův Týnec, **2018**.
[18] Suceska, M. Calculation of Detonation Parameters by EXPLO5 Computer Program. *Mater. Sci. Forum* **2004**, 325-330.
[19] Wood, W.W.; Kirkwood, J. Diameter Effect in Condensed Explosives: the Relationship between Velocity and Radius of Curvature of the Detonation Wave. *J. Chem. Phys.* **1954**, *22*(11): 1920-1924.
[20] Kirby, I.J.; Leiper, G.A. A Small Divergent Detonation Theory for Intermolecular Explosives. *Int. Detonation Symposium*, *Proc., 8th,* Naval Surface Weapons Center, White Oak, Silver Spring, MD, **1985**, 176-186.
[21] Esen, S.; Souers, P.C.; Vitello, P. Prediction of the Non-ideal Detonation Performance of Commercial Explosives using the DeNE and JWL++ Codes. *Int. J. Numerical Methods in Engineering* **2005**, *64*: 1889-1914.
[22] Fried, L.E.; Howard, W.M.; Souers, P.C. *CHEETAH 2.0 User`s Manual*. LLNL Report UCRL-MA-117541, **1998**.
[23] Cooper, P.W. *Explosives Engineering*. New York, Wiley-WCH, Inc., **1996**.
[24] Dobratz, B.M. *LLNL Explosives Handbook*. DE85-015961, **1981**.
[25] Berman, H.A.; West, E.D. Heat Capacity of Liquid Nitromethane from 35 to 200 °C. *J. Chem. Eng. Data* **1969**, *14*: 107-109.
[26] Utkin, A.V.; Mochalova, V.M.; Garanin, V.A. Structure of Detonation Waves in Nitromethane and a Nitromethane/Methanol Mixture. *Combust., Expl., Shock Waves* **2012**, *48*(3): 350-355.
[27] Hobbs, M. L.; Bear, M. R. Calibrating the BKW-EOS with a Large Product Species Data Base and Measured C-J Properties. *Int. Detonation Symposium*, *Proc., 10th,* Office of Naval Research, Arlington VA, **1995**, 409-418

Received: December 19, 2019
Revised: June 19, 2020
First published online: June 25, 2020